Articles

Rapid Synthesis of Al-Containing Mesoporous Silica Hard Spheres of 30−50 μm Diameter

Katsunori Kosuge* and Puyam S. Singh†

Catalyst Development Group, Research Institute for Green Technology, National Institute of Advanced Industrial Science and Technology, 16-1 Onogawa, Tsukuba-shi, Ibaraki, 305-8569 Japan

Received July 27, 2000. Revised Manuscript Received May 14, 2001

Al-containing mesoporous silica hard spheres of 30−50 μm mean diameter have first been synthesized at room temperature in 80 min using 1-alkylamine as a structure-directing agent. The formation of the spheres occurs only within a definite range of molar synthesis compositions of Si, Al, HCl, H_2O, and 1-alkylamine, especially HCl molar concentration. Scanning electron microscopic observation and particle size analysis revealed that the spherical products obtained by octylamine templating resulted in a higher uniformity in particle size, and the addition of ethanol into the reaction mixture afforded even more uniform particle size distribution. Textural mesoporosity along with framework mesoporosity for the spheres was observed with octylamine templating, while no textural porosity was found for the spheres produced by other amines. The calcined spheres with a pore structure lacking long-range order have BET surface areas of over 800 m^2/g at 600 °C. The Al-containing silica spheres have medium-strength acid sites which are weaker than those usually present in zeolites.

Introduction

The syntheses of mesoporous materials with a controlled macroscopic morphology have recently received much attention[1] since the discovery of M41S products[2] with a well-ordered pore array in 1992. These hierarchical structured materials have at least two different scale length orderings: ordered mesopores on a nanometer scale and ordered morphogenesis of shapes on a micrometer scale designed by a supramolecular templating and an interfacial phenomenon, respectively. The diverse morphogenesis of shapes in this promising class of M41S materials will lead to new opportunities in numerous areas of application. Especially, it is noteworthy that mesoporous spheres could be directly used as packing materials in chromatography or as an easy-to-handle form for catalytic purposes.[3] Recently, the efficiency of nearly spherical mesoporous silica of 4−10 μm diameter has been reported in chromatographic applications and in particular for flash techniques, where particles with high surface area and capacity are required.[4] Such mesoporous spheres with larger, micrometer sizes and a definite morphology should be useful in future liquid-phase chromatography and fluidized-bed catalysis applications. Although a variety of spherical mesoporous silicas have been synthesized so far, almost all the silica spheres have been obtained by using a biphasic system of a quaternary ammonium surfactant with an additional auxiliary organic solvent and cosurfactant.[3,5−9] The diameter of those mesoporous silica spheres has been less than ca. 5 μm, excluding one example[6] where the sphere sizes were more than ca. 1 mm. Using a nonionic poly(ethylene oxide)-based surfactant, a silica sphere of less than 7 μm has been synthesized.[10] In all of the above syntheses, a relatively longer reaction time of 1−3 days[3,5−10] or hydrothermal

* To whom correspondence should be addressed. Telephone: +81-298-61-8492. FAX: +81-298-61-8459. E-mail: k.kosuge@aist.go.jp.

† Current address: CSIRO Manufacturing Science and Technology, Private Bag 33, Clayton South MDC, Vic. 3169, Australia.

(1) Linden, M.; Schacht, S.; Schüth, F.; Steel, A.; Unger, K. K. *J. Porous Mater.* **1998**, *5*, 177. Biz, S.; Occelli, M. L. *Catal. Rev.−Sci. Eng.* **1998**, *40*, 329. Ying, J. Y.; Mehnert, C. P.; Wong, M. S. *Angew. Chem., Int. Ed.* **1999**, *38*, 56. Ciesla, U.; Schüth, F. *Microporous Mesoporous Mater.* **1999**, *27*, 131.

(2) Kresge, C. T.; Leonowicz, M. E.; Roth, W. J.; Vartuli, J. C.; Beck, J. S. *Nature* **1992**, *359*, 710. Beck, J. S.; Vartuli, J. C.; Roth, W. J.; Leonowicz, M. E.; Kresge, C. T.; Schmitt, K. D.; Chu, C. T.-W.; Olson, D. H.; Sheppard, E. W.; McCullen, B.; Higgins, J. B.; Schlenker, J. L. *J. Am. Chem. Soc.* **1992**, *114*, 10834.

(3) Grün, M.; Lauer, I.; Unger, K. K. *Adv. Mater.* **1997**, *9*, 254. Büchel, G.; Unger, K. K.; Matsumoto, A.; Tatsumi, K. *Adv. Mater.* **1998**, *10*, 1036.

(4) Gallis, K. W.; Araujo, J. T.; Duff, K. J.; Moore, J. G.; Landry, C. C. *Adv. Mater.* **1999**, *11*, 1452.

(5) Schacht, S.; Huo, Q.; Voigt-Martin, I. G.; Stucky, G. D.; Schüth, F. *Science* **1996**, *273*, 768.

(6) Huo, Q.; Feng, J.; Schüth, F.; Stucky, G. D. *Chem. Mater.* **1997**, *9*, 14.

(7) Yang, H.; Vovk, G.; Coombs, N.; Sokolov, I.; Ozin, G. A. *J. Mater. Chem.* **1998**, *8*, 743.

(8) Qi, L.; Ma, J.; Cheng, H.; Zhao, Z. *Chem. Mater.* **1998**, *10*, 1623.

(9) Lin, H. P.; Cheng, Y. R.; Mou, C. Y. *Chem. Mater.* **1998**, *10*, 3772.

10.1021/cm000623b CCC: $20.00
Published on Web 07/17/2001

Table 1. Representative Products Obtained under Different Reaction Conditions

run no.	Si,[a] mol	Al,[b] mol	1-alkylamine, mol (carbon no.)	HCl, mol	H_2O, mol	stirring speed, rpm	S_{BET}, $m^2\ g^{-1}$	V,[c] $mL\ g^{-1}$	morphology
1	1	0.027	0.339 (8)	0.084	37.31	600	901	0.39	spheres
2	1	0.023	0.344 (10)	0.085	37.86	600			aggregated solids[d]
3	1	0.024	0.345 (12)	0.085	38.04	600			aggregated solids[d]
4	1	0.038	0.344 (8)	0.085	37.90	600	858	0.34	spheres
5	1	0.042	0.343 (8)	0.085	37.84	600	866	0.33	monolith
6	1	0.025	0.342 (8)	0.068	37.71	600	916	0.43	spheres[e]
7	1	0.023	0.344 (8)	0.102	37.89	600	831	0.39	no distinct morphology
8	1	0.023	0.341 (8)	0.056	25.02	600	970	0.31	cluster of spheres
9	1	0.023	0.275 (8)	0.085	37.90	600	937	0.38	irregular solid block
10	1	0.023	0.478 (8)	0.085	37.63	600	1038	0.25	cluster of spheres
11	1	0.023	0.400 (10)	0.014	31.47	600	1012	0.95	spheres
12	1	0.024	0.398 (12)	0.006	31.75	600	968	1.12	spheres[e]
13	1	0.023	0.493 (12)	0.006	31.47	600	985	1.01	spheres

[a] Tetraethyl orthosilicate (TEOS). [b] Aluminum tri-*sec*-butoxide. [c] Pore volume excluding the textural pore volume determined by *t*-plot analysis. [d] Aggregated solids which consist of small spherical particles with various sizes. [e] Agglomerated spheres with less homogeneity in the diameter.

conditions[4] have been needed to prepare those previous silica spheres, some of which were hollow spheres[5,9] with less advantageous mechanical strengths for the usual applications. Furthermore, metal-substituted mesoporous silica hard spheres of several tens of micrometers in diameter in which Si^{4+} is isomorphously substituted by other metal ions in the silicate framework have not been reported.

In the course of our investigations using 1-alkylamine as a structure-directing agent,[11] we have obtained an aggregation of 1-alkylamine-containing colloidal mesostructured solid particles that can be useful for synthesizing new Al-containing mesoporous silica hard spheres of 30−50 μm mean diameter. These spheres can be produced at room temperature in a reaction time of 80 min. This aggregation process of colloidal mesostructured particles is the only method for producing mesoporous hard spheres with a mean diameter of several tens of micrometers.

Experimental Section

Synthesis. The Al-containing mesoporous silica spheres have been synthesized by using 1-alkylamine (designated C8 for octylamine, C10 for decylamine, and C12 for dodecylamine) as template and tetraethyl orthosilicate (TEOS) and aluminum-tri-*sec*-butoxide as inorganic framework sources. The TEOS, aluminum-tri-*sec*-butoxide, and 1-alkylamine were mixed for 10−20 min with stirring at a definite rate, and then aqueous HCl was rapidly added to this homogeneous solution while stirring was continued for another 60 min. Every commercial chemical was used without any purification. The reaction conditions and molar ratio of the reactants with respect to Si in every suspension are given in Table 1. The solid products were obtained in one quick step for a very short time within 80 min at room temperature. The resultant products were collected by filtration, dried at 50 °C for 2 days, and calcined in static atmosphere at over 600 °C for 1 h.

Characterization. Scanning electron microscopic (SEM) images were obtained on a JEOL5300, and transmission electron microscopic (TEM) images were observed on a JEOL 2000FX. A cross-sectional magnified TEM image was obtained by embedding the sample in epoxy resin and cutting into thin sections of ca. 0.1 μm thickness. The distribution of Al atoms in the silica matrix was analyzed by time-of-flight secondary ion mass spectrometry (TOF-SIMS) using TRIFT II. This image was observed for the sample prepared by embedding in epoxy resin and then cross sectioned.

Particle size distribution was analyzed using a Coulter Multisizer IIe.

N_2 isotherms were obtained at −196 °C on a BELSORP 28 under continuous adsorption conditions. Prior to measurement, the samples were heated at 200 °C for 2 h and finally outgassed to 10^{-3} Torr at room temperature. BET and *t*-plot analysis were used to determine the total specific surface area (S_{BET}) and mesopore volume (V) of the products.[12] The mesopore size distributions were calculated by the Horvath−Kawazoe (HK) method.[13]

Powder X-ray diffraction (XRD) patterns were obtained with a Rigaku Rotaflex diffractometer equipped with a rotating anode and using Cu Kα radiation.

Solid-state MAS NMR spectra were recorded on a CMX 300 MHz NMR spectrometer using 7.5 mm zirconia rotors for ^{29}Si and 4 mm for ^{27}Al at 59.71 MHz. The sample spinning frequency for the ^{29}Si MAS NMR measurements was 3 kHz using 90° pulses at 600 s intervals with high power proton decoupling. The ^{29}Si CP MAS NMR spectra were recorded using a 4 ms contact time, a 5 s recycling delay time, and 2000 scans. The ^{27}Al solid-state MAS NMR spectra were measured using 4.0 mm zirconia rotors spinning at 12 kHz using 90° pulses at 180 s intervals with high power proton decoupling. Prior to the ^{27}Al MAS NMR experiments, all calcined samples were kept for 48 h in air at room temperature.

NH_3 TPD Analysis. The acidic properties of the products were examined using the temperature programmed desorption (TPD) of ammonia. About 0.1 g of the calcined samples at 600 °C was outgassed after heating at 500 °C for 1 h in an He flow. The evacuated sample was equilibrated with NH_3 (100 Torr) at 100 °C for 30 min and subsequently evacuated at 100 °C for 1 h. By increasing the temperature at a constant rate of 10 °C/min, the NH_3 TPD spectra were detected by a mass spectrometer. Furthermore, the TPD spectra were obtained after removal of physisorbed NH_3 by treatment at 180 °C in an He flow for 30 min.[14] The TPD spectra for the proton ZSM-5 sample with ca. 2 mol % Al for Si, of which the amount of NH_3 desorbed was 1.11 mmol/g, were also measured to assign the TPD peaks and to estimate the acid amount of the spheres.

Results and Discussion

SEM Observation. Table 1 lists the representative reaction conditions with a description of the morphology in which the Al-containing mesoporous silicas were

(10) Boissière, C.; van der Lee, A.; El Mansouri, A.; Larbot, A.; Prouzet, E. *Chem. Commun.* **1999**, 2047.

(11) Singh, P. S.; Kosuge, K. *Chem. Lett.* **1998**, 110; *Chem. Lett.* **1998**, 130.

(12) Sing, K. S. W.; Everett, D. H.; Haul, R. A. W.; Moscou, L.; Pierotti, R. A.; Rouquerol, J.; Siemienewska, T. *Pure. Appl. Chem.* **1985**, *57*, 603.

(13) Horvath G.; Kawazoe, K. *J. Chem. Eng. Jpn.* **1983**, *16*, 470.

(14) Aguado, J.; Serrano, D. P.; Romero, M. D.; Escola, J. M. *Chem. Commun.* **1996**, 725.

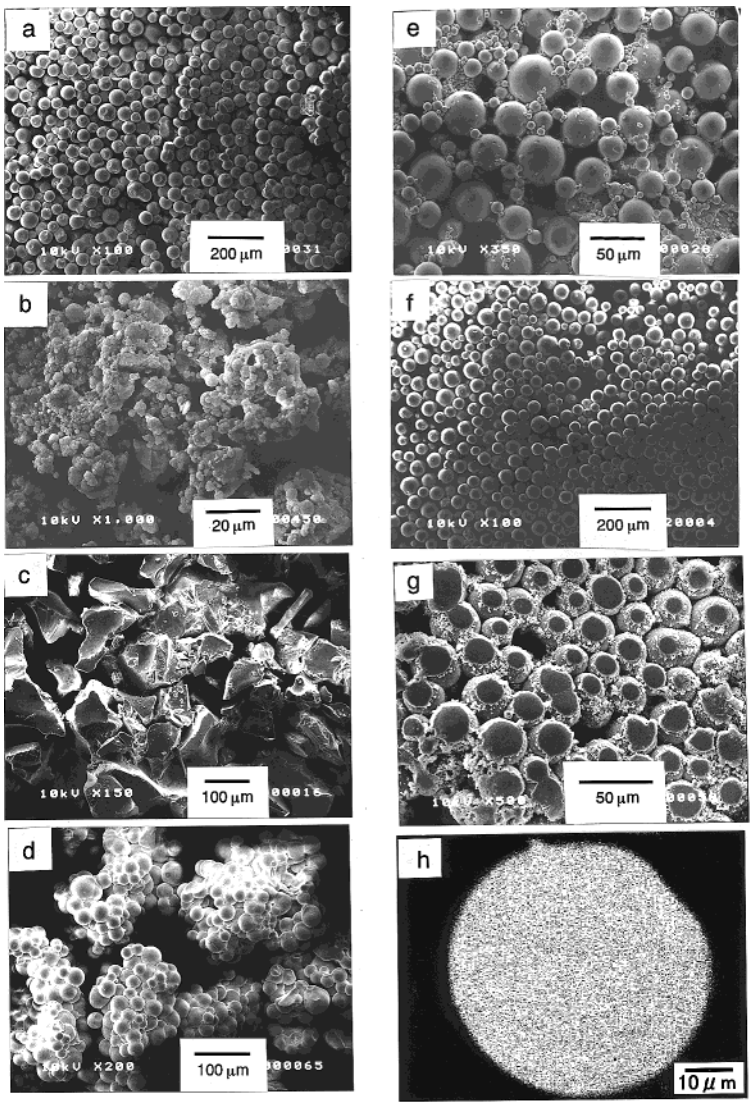

Figure 1. SEM images of calcined products at 600 °C obtained from (a) run 1, (b) run 3, and (c) run 5 in Table 1, (d) obtained with higher stirring rate at 1200 rpm using almost the same reactants mixing ratio as that for run 1, (e) obtained from run 12, and (f) the product obtained by the addition of ethanol into the reaction mixture of run 12. (g) SEM micrograph of the product corresponding to run 1, which was mounted directly on the SEM sample holder 1.5 min after the addition of HCl, and (h) cross-sectional TOF-SIMS image indicating the homogeneous distribution of Al atoms in the sphere corresponding to run 1 as shown by the bright spots.

obtained. In this table the effect of various synthetic parameters on the morphology has been described, using, for example, C8 templated products. The limited Al-containing mesoporous silicas were illustrated for C10 and C12 templating, while a number of products were synthesized under a variety of reaction conditions. Figure 1 shows the SEM images of the representative calcined Al-containing mesoporous products. At almost the same mixing ratio of the reactants under which the uniform spherical morphology can be observed in C8 templating, as shown in Figure 1a (run 1), the products obtained using longer alkyl chain amines in run 2 (C10) and 3 (C12) are aggregated solids consisting of small spherical particles with various sizes, as shown in Figure 1b. It was found that the formation of the monodispersed Al-containing mesoporous spherical silicas places severe restrictions on the various parameters such as HCl concentration and amount of Al, H_2O, and 1-alkylamines in the starting mixture. The spherical morphology observed is completely destroyed with a higher content of Al (run 5; Figure 1c) and higher HCl concentration (run 7). On the other hand, a higher stirring rate at 1200 rpm led to agglomeration between the spherical particles as shown in Figure 1d, indicating that the stirring rate and therefore shear fluid flow have a smaller effect on the spherical morphology in contrast to others,[5−9,15] although the diameter of the spheres decreased slightly with the higher rate.

Furthermore, among the 1-alkylamines large differences in the HCl concentration were used to synthesize monodispersed spherical particles. By optimizing the HCl concentration and amine volume, such spheres have been obtained for C10 (run 11) and C12 (run 12 and run 13) templating as shown in Table 1. However, there are many smaller particles among the larger particles of those products as shown in Figure 1e (run 12). It can be seen that, by the addition of an auxiliary

(15) Lin, H. P.; Kao, C. P.; Mou, C. Y.; Liu, S. B. *J. Phys. Chem. B* **2000**, *104*, 7885.

solvent such as alcohol, there is a decrease in the population density of the smaller particle sizes resulting in more uniformity in larger particle size distributions as shown in Figure 1f. The products were synthesized with the addition of 0.49 mol of ethanol with respect to Si to the reaction mixture of run 12. Such a remarkable improvement of the spherical morphology has not been previously observed, although the effect of the ethanol addition in the synthesis mixture on the morphological change in the product was reported for the synthesis of mesoporous silica.[15−18]

Our rapid synthesis of mesostructured hard spheres should be due to the initial formation of a neutral S°I° assembly by the mixed alkoxides and 1-alkylamine solution[21] and then the immediate nucleation of a $S^+X^-I^+$ assembly by addition of aqueous HCl with a Coulombic interaction between the charged species: protonated amine (S^+), coordinating anions of Cl^- (X^-), and positively charged silica−alumina oligomer (I^+).[11] The development of the $S^+X^-I^+$ assembly would proceed in the formation of the primary particles, the growth of which should yield spherical products. It is well-known that the differences in the nucleation and growth rates are dependent factors for monodispersed particle formation, indicating that the higher degree of separation between nucleation and the growth process leads to more monodispersed particles.[16,19,20] The addition of ethanol leads to lower polarity of the solvent, which results in slower nucleation and growth of the mesostructured products because of the slower TEOS hydrolysis and mesostructure assembly [16] and, in addition, the formation of the shorter self-assembled micelles.[15] These factors would result in a higher degree of such separation and lead to easier formation of monodispersed spherical particles in longer chain alkylamines as shown in Figure 1f.

On the other hand, the SEM picture of the product corresponding to run 1 which was mounted directly on the sample holder 1.5 min after the addition of aqueous HCl shows a beautiful array of loosely packed micrometer-sized spheres in the midst of many other small nanometer-sized primary particles, as shown in Figure 1g. However, such small particles cannot be observed in the final spherical product, as shown in Figure 1a. In addition, the cross-sectional TOF-SIMS image of the final product reveals that Al atoms are distributed homogeneously in the spherical product, as shown in Figure 1h. These observation results including a cross-sectional magnified TEM image not presented here indicate that the final micrometer-sized hard spherical product would be the aggregate of nanometer-sized primary colloidal particles due to a well-known aggregation mechanism.[10,19]

Since the aim of this work is to describe the Al-containing mesoporous silica hard spheres with 30−50 μm mean diameter synthesized by a simple route using 1-alkylamines as a template, the spherical products will be mainly characterized below.

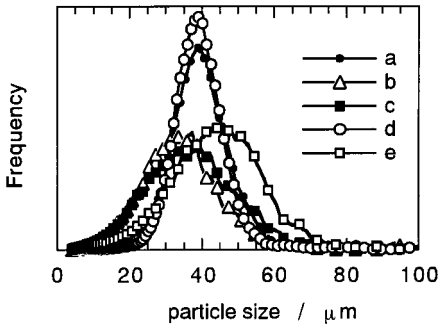

Figure 2. Particle size distribution of the products obtained using different 1-alkylamines: (a) octylamine (run 1), (b) decylamine (run 11), and (c) dodecylamine (run 13). (d) and (e) show the effect of the ethanol addition on the particle size distribution for octylamine and dodecylamine templating in run 1 and run 12, respectively.

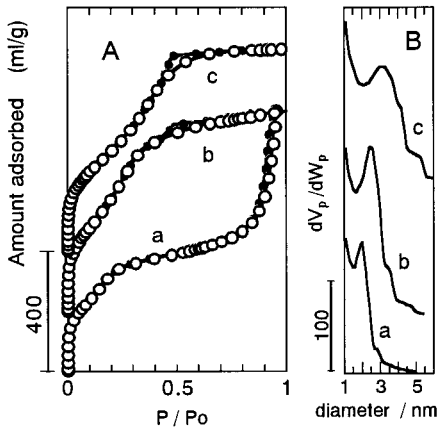

Figure 3. (A) N_2 adsorption−desorption isotherms of the monodispersed spheres of (a) run 1 (C8), (b) run 11 (C10), and (c) run 13 (C12) in Table 1. (B) Pore size distribution curves of the corresponding products as shown in (A).

Particle Size Distribution. Figure 2 shows the representative particle size distribution curves based on volume. The mean particle size of the product (run 1) obtained from the synthesis using C8 is ca. 38.2 μm. The spheres synthesized using different 1-alkylamines have a mean particle size of 30.2 μm for C10 (run 11) and 32.0 μm for C12 (run 12), while the size distribution is broader with increasing alkyl chain length. These results are consistent with SEM observations. From the comparison of the curves of run 12 with and without ethanol in which C12 was used as template, it can be seen that the particle size distribution curve becomes sharper with increasing particle size at 39.9 μm for the product obtained from the reaction mixture containing 0.49 mol of ethanol. In the case of the C8 templating with 1.16 mol of ethanol, the particle size distribution curve also becomes sharper while no change in the mean particle size occurs, as shown in Figure 2.

Nitrogen Adsorption and Desorption Isotherms. Figure 3A shows the N_2 adsorption−desorption isotherms for the monodispersed spheres obtained for the different carbon numbers of 1-alkylamines used as templates, and the corresponding pore size distribution curves based on the HK method are presented in Figure 3B. The adsorption step based on the filling of the

(16) Zhang, W.; Pauly, T. R.; Pinnavaia, T. J. *Chem. Mater.* **1997**, *9*, 2491.
(17) Anderson, M. T.; Martin, J. E.; Odinek, J. G.; Newcomer, P. P. *Chem. Mater.* **1998**, *10*, 311.
(18) Pauly, T. R.; Liu, Y.; Pinnavaia, T. J.; Billinge, S. J. L.; Rieker, T. P. *J. Am. Chem. Soc.* **1999**, *121*, 8835.
(19) Ocaña, M.; Rodriguez-Clemente, R.; Serna, C. J. *Adv. Mater.* **1995**, *7*, 212.
(20) Sugimoto, T. *Adv. Colloid Interface Sci.* **1987**, *28*, 65. Matijeviæ, E. *Chem. Mater.* **1993**, *5*, 412.
(21) Tanev, P. T.; Chibwe, M.; Pinnavaia, T. J. *Nature* **1994**, *368*, 321.

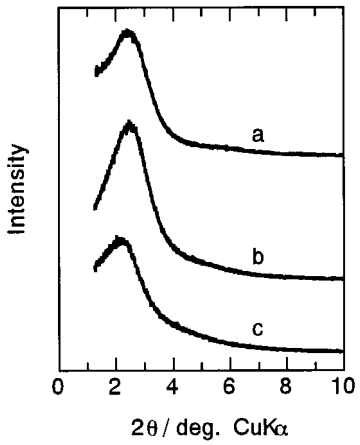

Figure 4. XRD patterns of the spherical products of (a) run 1, (b) run 11, and (c) run 13 in Table 1.

framework mesopores are observed in the C8 product at relative pressures of ca. 0.1, which exhibit the pore size distribution curve with mean pore diameters of ca. 2 nm, as shown in Figure 4. The isotherms of every product for C8 exhibited a pattern similar to that of Figure 3a irrespective of the difference in the macroscopic morphology, indicating no significant effect of the synthesis conditions on the porous properties. The BET surface areas (S_{BET}) and mesopore volume (V) are given in Table 1, showing a high S_{BET} of over 800 m^2/g for every calcined product at 600 °C. The steep increase at higher relative pressures is attributed to additional textural mesopores, which afford a higher catalytic activity.[18] The S_{BET}, and pore volume (V), of the calcined product in run 1 decreases with increasing calcination temperature, from 901 m^2/g ($V = 0.39$) at 600 °C to 763 m^2/g ($V = 0.28$) at 800 °C, to 567 m^2/g ($V = 0.15$) at 900 °C, and to 114 m^2/g ($V = 0$) at 1000 °C. With SEM observation and particle size distribution analysis, morphological change was not observed even at 1000 °C. Moreover, the hysteresis loop in the isotherm as shown in Figure 3a was still detected at 1000 °C, indicating the retention of textural pores even after the framework pores have collapsed.

Compared to the isotherms of the sphere obtained by C8 templating, the isotherms of the spherical products by C10 and C12 templating have little textural mesoporosity between the particles, indicating that most of the S_{BET} is attributed to the framework mesopores. The mesopore size of the spheres is ca. 2.6 nm for the C10 template and ca. 3.3 nm for the C12 template. However, the isotherms of the products in run 2 and run 3 synthesized under almost the same mixing ratio of the reactants as that for run 1 exhibited a similar steep increase at higher relative pressures attributed to additional textural mesopores. On the other hand, there is no significant change in the shape of the isotherms of the products obtained from the reaction mixture containing ethanol under the experimental study investigated, indicating no influence from ethanol addition on the mesoporosity of the products.

Powder XRD Data. The X-ray diffraction (XRD) patterns of all of the calcined spheres at 600 °C in this study show an intense peak at a d spacing of ca. 3.6−4.0 nm along with a weak broad shoulder (Figure 4). These properties are characteristic of mesoporous materials with a pore structure lacking long-range order

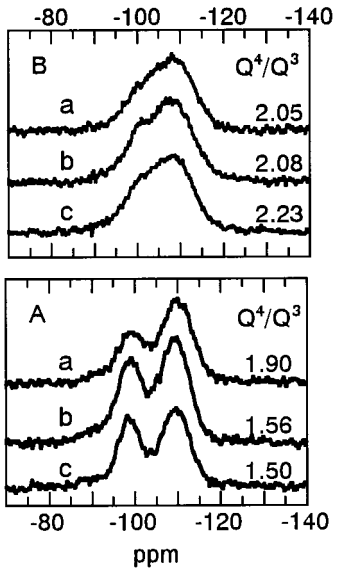

Figure 5. ^{29}Si MAS NMR spectra of (A) as-synthesized and (B) calcined spherical products at 600 °C corresponding to (a) run 1, (b) run 11, and (c) run 13 in Table 1.

such as those of the HMS[21] and MSU-1[22] samples. The d spacing in the sphere of C8 is larger than that of C10, indicating that the sphere prepared using decylamine should have thinner pore walls than the others. Also, there is a bigger difference than expected in the d spacing between the samples of C10 and C12. It has been reported[23] that in various types of pathways to prepare mesoporous silica the d spacing and the corresponding pore wall thickness do not necessarily shift toward larger and smaller ones, respectively, as the alkyl chain length used as a templating agent is longer. Especially it has also been observed that the d spacing in the C8 sample is larger than that of C10 in 1-alkylamine templating.[23]

^{29}Si MAS NMR. Figure 5 shows the ^{29}Si MAS NMR spectra for as-synthesized and corresponding calcined spherical products. The spectra of the as-synthesized products clearly exhibit two well-resolved peaks at chemical shifts of −100 and −110 ppm, and weak shoulders at −90 ppm. These can be assigned to the Q^3 [$Si(OSi)_3(OH)$], Q^4 [$Si(OSi)_4$], and Q^2 [$Si(OSi)_2(OH)_2$] structural units, respectively.[24] The spectrum of the as-synthesized sample by C8 templating reveals a much larger Q^4/Q^3 ratio (1.90), i.e, a much more highly cross-linked framework than the samples obtained using other amines. On the other hand, it was important to note that the Q^4/Q^3 ratio for the as-synthesized products obtained by almost the same mixing ratio of the reactants (run 1, run 2, and run 3) was the same value irrespective of the alkyl chain length. Furthermore, the comparison of the ^{29}Si MAS NMR spectra of the as-synthesized and calcined spherical samples emphasizes the difference between the 1-alkylamines. The enhancement in the cross-linking of the silicate framework by calcination is larger for the products obtained for a longer alkyl chain length of C10 and C12 than that for C8.

(22) Bagshaw, S. A.; Prouzet, E.; Pinnavaia, T. J. *Science* **1995**, *269*, 1242.
(23) Tanev, P. T.; Pinnavaia, T. J. *Chem. Mater.* **1996**, *8*, 2068.
(24) Engelhardt, G.; Michel, D. *High-Resolution Solid-State NMR of Silicates and Zeolites*; John Wiley: New York, 1987.

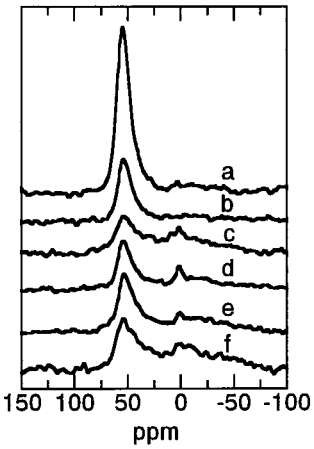

Figure 6. ^{27}Al MAS NMR spectra of (a) and (b) as-synthesized product obtained from run 5 and run 1. The others are for calcined products at 600 °C of (c) run 5, (d) run 1, (e) run 11, and (f) run 13, respectively.

From the above experimental results, the variations in the Q^4/Q^3 ratio in the ^{29}Si MAS NMR spectra, the particle size distribution, the porosity, and XRD patterns have been observed for the spherical products obtained under the different 1-alkylamine templatings. It should be noted that the spherical products obtained using different 1-alkylamines have been synthesized at different HCl concentrations and volumes of amine, as shown in Table 1. It is well-known that the alkyl chain conformations, the degree of micelle packing, and the degree of framework cross-linking depend on the combination of the following factors: (i) the pH conditions, (ii) the surfactant and inorganic reagent concentrations, (iii) the type of ions present in the reaction mixture, and (iv) the ionic strength of the solution.[15−17,23] Hence, the variations as described above would be attributed to differences in the hydrolysis rates of inorganic species under the different amine templatings.

^{27}Al MAS NMR. Figure 6 shows the ^{27}Al MAS NMR spectra of the representative as-synthesized and calcined products. Before calcination, only an intense line can be detected at ca. 55 ppm from four-coordinate structural aluminum,[25] indicating that the Al contained in the products has been incorporated into the silicate framework of the product even at the higher Al content of the monolith morphology. Unlike that of the as-synthesized products, every calcined material at 600 °C has a weak broad line at ca. 0 ppm due to the six-coordinate extraframework Al,[25] in addition to the line at ca. 55 ppm. This indicates that Al atoms are incorporated as isolated Al sites into the silicate framework in the as-synthesized materials, while additional small amounts of the alumina phase were formed in the silica matrix upon calcination.

NH_3 TPD. Figure 7 shows the TPD spectra of the Al-containing silica spheres along with the ZSM-type zeolite before and after removal of physisorbed NH_3. The zeolite has two TPD peaks (Figure 7a), which are well-known as an l-peak (lower temperature peak) due to physisorbed NH_3 and an h-peak (higher temperature peak) ascribed to the ammonium cation bonded to the acid site.[14,26] The l-peak is almost completely removed during heating at 180 °C after NH_3 adsorption, while the h-peak is not affected (Figure 7b). Al-containing silica spheres show the peak at ca. 250 °C even after the removal of the physisorbed NH_3, accompanied by a shoulder peak at ca. 480 °C (Figure 7c,d). The former peak should be ascribed to the Al atoms in the framework, indicating the presence of medium-strength acid sites in the Al-containing silica spheres.[14,27] These sites are weaker than those usually present in zeolites, of which TPD peaks appear at ca. 400 °C. Compared to the 1.11 mmol/g NH_3 desorbed for the ZSM-type zeolite between 245 and 550 °C, the amount of NH_3 desorbed for the spheres obtained from run 2 is 0.27 mmol/g between 155 and 410 °C. With increasing Al content, the amount of NH_3 desorbed becomes larger (0.43 mmol/g) although little change in the peak observed at higher temperature is seen (Figure 7e). These results indicate that the peak at ca. 500 °C for the spheres might be based on extraframework aluminum.[27]

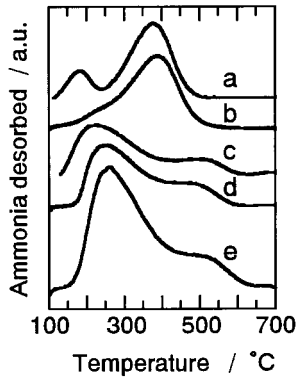

Figure 7. NH_3 TPD spectra of (a) the ZSM-type zeolite and (c) the calcined product at 600 °C obtained from run 1, and corresponding profiles (b) and (d) after the removal of the physisorbed NH_3 by heat treatment. (e) Spectra of the calcined product at 600 °C obtained from run 5 after the removal of the physisorbed NH_3.

Conclusions

Al-containing mesoporous silica hard spheres several tens of micrometers in diameter have been synthesized by use of 1-alkylamine as template and mixed Si and Al alkoxides as the inorganic framework source under acidic conditions. The spherical solids were obtained in one quick step in a very short time at room temperature due to the immediate formation of the $S^+X^-I^+$ assembly through the neutral S°I° assembly in a homogeneous solution. The 30−50 μm sized spherical products should consist of many nanometer-sized mesostructured particles. The formation of the spherical morphology is very dependent on the reactant concentrations and alkyl chain length of the 1-alkylamine. The spherical products obtained by octylamine templating produce a more uniform particle size distribution than the other amines, which also exhibit a textural mesoporosity retained even up to 1000 °C along with the framework mesopores. No textural porosity was observed for the products obtained using the other amines. Every calcined sphere has a

(25) Luan, Z.; Cheng, C. F.; He, H.; Klinowski, J. *J. Phys. Chem.* **1995**, *99*, 10590. Mokaya, R.; Jones, W. *J. Catal.* **1997**, *172*, 211.

(26) Miyamoto, T.; Katada, N.; Kim, J. H.; Niwa, M. *J. Phys. Chem.* **1998**, *102*, 6738.

(27) Okumura, K.; Nishigaki, K.; Niwa, M. *Chem. Lett.* **1998**, 577. Kosslick, H.; Lischke, G.; Parlitz, B.; Storek, W.; Fricke, R. *Appl. Catal., A: Gen.* **1999**, *184*, 49.

disordered wormhole-like pore structure and has a high BET surface area of over 800 m^2/g at 600 °C. The mesopore size of the spheres was changed by the alkyl chain length, which was ca. 2 nm for octylamine, ca. 2.5 nm for decylamine, and ca. 3.3 nm for dodecylamine, respectively. The Al-containing silica spheres have medium-strength acid sites that are weaker than those usually present in zeolites.

This simple and very fast process can be utilized for the synthesis of the other metal-containing mesoporous silica spheres of several tens of micrometers in diameter, such as Ti and Zr, the starting synthesis precursor alkoxides of which are stable in liquid phase at room temperature. Our procedure using 1-alkylamine as a structure-directing agent has been the only method for producing mesoporous hard spheres with a definite diameter of several tens of micrometers, which have never been synthesized. These new spheres should be promising porous materials for use as molecular sieves, adsorbents, and catalysts, especially for applications in future liquid-phase chromatography and fluidized-bed catalysis.

Supporting Information Available: Cross-sectional views of two magnified TEM images (images A and B) of a spherical particle in run 2, Figure 1a. This material is available free of charge via the Internet at http://pubs.acs.org.

CM000623B